A Rapid and Automatic MRF-Based Clustering Method for SAR Images

Gui-Song Xia, Chu He, and Hong Sun, *Member, IEEE*

***Abstract*—This letter presents a precise and rapid clustering method for synthetic aperture radar (SAR) images by embedding a Markov random field (MRF) model in the clustering space and using graph cuts (GCs) to search the optimal clusters for the data. The proposed method is optimal in the sense of maximum *a posteriori* (MAP). It automatically works in a two-loop way: an outer loop and an inner loop. The outer loop determines the cluster number using a pseudolikelihood information criterion based on MRF modeling, and the inner loop is designed in a "hard" membership expectation–maximization (EM) style: in the E step, with fixed parameters, the optimal data clusters are rapidly searched under the criterion of MAP by the GC; and in the M step, the parameters are estimated using current data clusters as "hard" membership obtained in the E step. The two steps are iterated until the inner loop converges. Experiments on both simulated and real SAR images test the performance of the algorithm.**

***Index Terms*—Graph cuts (GCs), image clustering, Markov random field (MRF) model, synthetic aperture radar (SAR).**

I. Introduction

WITH MORE and more synthetic aperture radar (SAR) sensors being used, the volume of SAR images rapidly increases. To effectively make use of these huge image data, fast and unsupervised image analysis algorithms will be very helpful and crucial. Motivated by these, this letter suggests a clustering method for SAR images, which rapidly and automatically works.

Clustering is a widely used approach for data analysis in feature space and can be applied to image segmentation, where it is also named unsupervised image segmentation. However, due to the assumption that pixels are spatial independent in the image space, the classical clustering methods [e.g., K-means and fuzzy c-mean (FCM)] and their variations [1] fail on SAR images, which have very low "SNR" because of their typical speckle signals.

A Markov random field (MRF) model provides an effective technique to impose local spatial information. Unsupervised MRF (USMRF)-based segmentation methods combine the local spatial information with the model-based clustering approach [2]–[8] and can increase the segmentation precision. However, the MRF-based methods always convert the segmentation problem to a combinational optimization task, which is computationally expensive, even by using some accelerating scheme [e.g., simulated annealing (SA)]. Thus, many MRF-based clustering methods are a tradeoff between the accuracy and the computational complexity of the segmentation.

Aiming at both improving the clustering accuracy and easing the computational burdens, this letter suggests a clustering method for SAR images by embedding an MRF model in the image space of the classical clustering methods, and using a recent multilevel graph cut (GC) [9]–[11] algorithm to effectively compute the optimal clusters for the data. The proposed algorithm works in a two-loop way: an outer loop and an inner loop. The outer loop determines the cluster number using a pseudolikelihood information criterion (PLIC) for MRF modeling. In addition, the inner loop is designed in a "hard" membership expectation–maximization (EM) style: in the E step, with fixed parameters, the optimal data clusters are rapidly searched under the criterion of maximum *a posteriori* (MAP) by the GC; and in the M step, the parameters are estimated using current data clusters obtained in the E step with "hard" cluster membership. The two steps are iterated until the two loops converge, respectively. To justify the efficiency of the proposed clustering approach, we compare it with traditional USMRF-based SAR image segmentation method and the classical clustering method, i.e., K-means.

The remainder of this letter is organized as follows. In Section II, the basics of the clustering criterion for SAR images are recalled and summarized. The multilevel GC algorithm is briefly described in Section III, and the proposed clustering method is presented in Section IV. In Section V, experimental results on real and simulated SAR images are presented and analyzed. Section VI gives our conclusion.

II. Clustering Criterion for SAR Images and MRF

In this section, first, with the assumption that the cluster number K is known, we recall the clustering criterion for SAR images. A SAR image on a rectangular pixel lattice S, containing a set of pixels $Y = \{y_s, s \in S\}$, will be summarized into K clusters, with the kth cluster modeled by some parameter $\boldsymbol{\theta}_k$. Thus, the entire set of clusters can be described by $\Theta = \{\boldsymbol{\theta}_k, k = 1, 2, \ldots, K\}$, and every pixel y_s will be assigned a cluster label $x_s \in \{1, 2, \ldots, K\}$. Let $X = \{x_s, s \in S\}$ denote the labeled image, and $W = (X, \Theta)$ denote a world state of the observed image Y. Therefore, the clustering is to pursue W,

Manuscript received December 6, 2006; revised March 7, 2007. This work was supported in part by the National Nature Science Foundation of China under Project 60372057 and Project 4037605 and in part by the Open Research Fund of the State Key Laboratory of Information Engineering in Surveying, Mapping and Remote Sensing.

The authors are with the Signal Processing Laboratory, Department of Communication Engineering, Electronic Information School, Wuhan University, Wuhan 430079, China (e-mail: gsxia.lhi@gmail.com; hc@eis.whu.edu.cn; hongsun@whu.edu.cn).

Color versions of one or more of the figures in this paper are available online at http://ieeexplore.ieee.org.

Digital Object Identifier 10.1109/LGRS.2007.903065

given the SAR image data Y, according to minimizing some criterion function $J(W,Y)$, i.e.,

$$\widehat{W} = \arg\min_{W} J(W,Y). \tag{1}$$

The clustering method based on maximum-likelihood estimate (MLE) formulates $J(W,Y)$ as

$$J(W,Y) = -\log\left(P(Y|X,\Theta)\right) \tag{2}$$

where $P(Y|X,\Theta)$ is the conditional probability of Y, given X and Θ. For instance, K-means and FCM are the classical MLE-based clustering methods.

Without considering the spatial relationship between adjacent pixels, the MLE-based methods are context free. That is to say, they take the labeled image as unified distribution. Therefore, the MLE-based methods generally cannot obtain good clustering results on SAR images because of the typical speckle signals in the images. To deal with SAR images, the cluster methods based on the criterion of MAP are usually used, which formulate $J(W,Y)$ as

$$J(W,Y) = -\log\left(P(Y|X,\Theta')\right) - \log\left(P(X,\lambda)\right) \tag{3}$$

where $P(X,\lambda)$ is a prior probability on X, λ is the parameter for modeling X, and $\Theta = \{\Theta', \lambda\}$. An effective prior knowledge is the spatial consistency in the labeled image space, which can be conveniently described by an MRF model [2], [3] as

$$P(X = x, \lambda) \propto \exp\left\{\lambda \sum_{c\in C} V_c(X)\right\} \tag{4}$$

where C is the clique set defined on the neighborhood system ∂x, and $V_c(x)$ is the potential function on clique c. In this way, the spatial relationship between adjacent pixels in the labeled image X is plugged in the clustering process of the observed image data Y.

On the other hand, it is well known that the Gamma distribution provides a good model for SAR intensity data [14]. Therefore, we suppose that each pixel of SAR image y_s is conditionally independent of all other pixels, conditioned on the knowledge of cluster label at that pixel x_s and satisfies gamma distribution. Formally, we have

$$P(Y|X,\Theta') = \prod_{s\in S} P(y_s|x_s,\sigma_{x_s}) \tag{5}$$

$$P(y_s|x_s,\sigma_{x_s}) = \frac{1}{\Gamma(L)}\left(\frac{L}{\sigma_{x_s}}\right)^{L} y_s^{L-1}\exp\left\{-\frac{Ly_s}{\sigma_{x_s}}\right\} \tag{6}$$

where L is the number of looks of the SAR image, and the parameters $\Theta' = \{\sigma_i, i = 1,2,\ldots,K\}$.

In this letter, to handle the spatial information in the labeled image, we use the Potts model [15], i.e.,

$$P(X = x, \lambda) \propto \exp\left\{\lambda \sum_{\{p,q\}\in C} V_{pq}(x_p, x_q)\right\} \tag{7}$$

with $V_{pq}(x_p,x_q) = 1$, for $x_p \neq x_q$, and $V_{pq}(x_p,x_q) = 0$ otherwise. The parameter λ expresses the degree of spatial homogeneity in X. $\lambda < 0$ means that neighboring pixels in X tend to be similar, whereas $\lambda > 0$ would mean that neighboring pixels tend to be dissimilar. If $\lambda = 0$, then the pixels in X are independent, and $P(X = x, \lambda)$ tend to be a uniform distribution. In (7), the sum is over all neighbor pairs $\{p,q\}$. This leads to the following conditional distribution:

$$P(x_s = k, |\partial x, \lambda) = \frac{\exp\left\{\lambda \sum_{x_t\in\partial x_s} V_{ts}(x_t,k)\right\}}{\sum_{m=1}^{K}\exp\left\{\lambda \sum_{x_t\in\partial x_s} V_{ts}(x_t,m)\right\}}. \tag{8}$$

Therefore, in this letter, the clustering criterion on a SAR image can be written as

$$J(W,Y) = \sum_{s\in S}\left\{L\log\sigma_{x_s} - (L-1)\log y_s + \frac{Ly_s}{\sigma_{x_x}}\right\} - \lambda \sum_{\{p,q\}\in C} V_{pq}(x_p,x_q). \tag{9}$$

III. Energy Minimization by the GCs

With a known cluster number K, the clustering method has to pursue the minimization of $J(W,Y)$, which can be taken as an energy minimization problem. Equation (9) shows that $J(W,Y)$ is nonconvex, and minimizing this energy is NP-hard [11]. Here, we use the GCs [9]–[11], a global optimization algorithm, to minimize $J(W,Y)$.

GC has been widely used in computer vision in the recent years and has become extremely popular for image segmentation.

The most effective GC algorithm for minimizing (9) is the α-expansion move algorithm [9]. For a cluster α and an arbitrary set $\beta \subset S$, we will define $x_s^{\beta\leftarrow\alpha} = \alpha$, if $s \in \beta$, and $x_s^{\beta\leftarrow\alpha} = x_s$ otherwise. That is to say, when we go from x to $x^{\beta\leftarrow\alpha}$, the pixels in the set β acquire the cluster α and all other pixels in S remain the same. This is called α-expansion move from x.

Reference [9] shows that the GCs can be used to efficiently find the best α-expansion move. The expansion move algorithm of [9] iteratively works: given an input labeling, it picks a cluster label α and uses the GCs to find the best α-expansion move, and moves to that cluster if it decreases the energy. The expansion move algorithm is actually an approximation algorithm, in which it guarantees that the solution lies within a constant factor of the global minimum. The constant factor is at least 2 and depends on the energy function. More details on this algorithm can be found in [9].

IV. Rapid and Automatic MRF (RAMRF) Clustering Algorithm

In this section, we detail the main proposed RAMRF embedded clustering method. First, we describe the PLIC, an approximation to Bayes factor (BF) [12], used to validate the cluster number of the image in this letter. Second, an effective scheme for parameter estimation and initialization is presented. Then, the main clustering algorithm is presented.

A. PLIC

One way to validate the cluster number is to use an approximate BF [13]. PLIC, which is proposed by Derek and

Adrian [12], is an approximation of BF based on the pseudo-likelihood for the MRF modeling.

Let $\widehat{W} = (\widehat{X}, \widehat{\Theta})$ with $\widehat{\Theta} = (\widehat{\Theta'}, \widehat{\lambda})$ be the estimation of W, given the cluster number K. Then, according to [12]

$$\mathrm{PLIC}(K) = 2\log\left(L_{\mathrm{MRF}}(Y|K)\right) - |\widehat{\Theta}|\log\left(|S|\right) \tag{10}$$

where $|f|$ is the cardinality of f, and $L_{\mathrm{MRF}}(Y|K)$, as shown as follows, is the pseudolikelihood of Y, given $\widehat{W}$ and K, based on the MRF modeling:

$$\begin{aligned} L_{\mathrm{MRF}}(Y|K) &= \prod_{s\in S} P(y_s|\partial\widehat{x}_s, \widehat{\Theta}, K) \\ &= \prod_{s\in S}\sum_{k=1}^{K} P(y_s|\widehat{x}_s = k, \widehat{\sigma}_k) P(\widehat{x}_s = k|\partial\widehat{x}_s, \widehat{\lambda}) \end{aligned} \tag{11}$$

where $P(y_s|\widehat{x}_s = k, \widehat{\sigma}_k)$ and $P(\widehat{x}_s = k|\partial\widehat{x}_s, \widehat{\lambda})$ are computed, respectively, by (6) and (8).

The PLIC adopts a sequential approach to choose K to maximize (10) [12]. It begins by computing $\mathrm{PLIC}(K)$ for $K = 1$, and then increases the value of K. At each step, as it incrementally increases K from $K-1$, it compares $\mathrm{PLIC}(K)$ with $\mathrm{PLIC}(K-1)$ and takes the first local maximum of $\mathrm{PLIC}(K)$ to be the choice for the number of clusters K.

B. Estimation of Θ

In the inner loop, the parameters $\Theta = (\Theta', \lambda)$, with $\Theta' = \{\sigma_k, k = 1, 2, \ldots, K\}$, must be estimated. According to (6), the MLE of σ_k can be written as

$$\widehat{\sigma}_k = \frac{\sum_{s\in S} y_s u(\widehat{x}_s, k)}{\sum_{s\in S} u(\widehat{x}_s, k)}, \qquad k = 1, 2, \ldots, K \tag{12}$$

where $u(i, j) = 1$ for $i = j$, and $u(i, j) = 0$ otherwise, and $\widehat{\Theta'} = \{\widehat{\sigma}_k, k = 1, 2, \ldots, K\}$.

To estimate λ from X, we use the algorithm proposed by Derin and Elliot [15], which needs not only to solve linear equations but also provide very accurate results.

C. Initialization of the Cluster Parameters

As an iterated approach, the RAMRF clustering method is sensitive to the initial cluster parameters Θ. Here, we present an effective parameter initialization scheme, according to minimizing the inner variance of the clusters.

We suppose the image Y to be summarized into K clusters, with the kth cluster written as $Y_k = \{y_s|x_s = k, s \in S\}$, where $k = 1, 2, \ldots, K$. Moreover, let $\widehat{\Theta}_K = \{\widehat{\sigma}_{1,K}, \widehat{\sigma}_{2,K}, \ldots, \widehat{\sigma}_{K,K}, \widehat{\lambda}_K\}$ denote the final estimation of Θ, and $var(Y_k)$ denote the variance of Y_k. Therefore, the scheme to obtain $\widehat{\Theta}_K^{(0)} = \{\widehat{\sigma}_{1,K}^{(0)}, \widehat{\sigma}_{2,K}^{(0)}, \ldots, \widehat{\sigma}_{K-1,K}^{(0)}, \widehat{\sigma}_{K,K}^{(0)}, \widehat{\lambda}_K^{(0)}\}$, the initial estimation of Θ, is as follows.

1) Find the cluster m from the $K-1$ clustering results, where $m = \arg\max_{\{1,2,\ldots,K-1\}} var(Y_k)$.
2) Sample in the mth cluster Y_m to establish two sets Δ_1 and Δ_2 for initializing parameters.
   (a) Randomly draw N, $N \geqslant 2$, samples $\{y_{S_1}, \ldots, y_{S_N}\}$ from Y_m.
   (b) Push $y_{\min} = \min\{y_{S_1}, \ldots, y_{S_N}\}$ into Δ_1 and $y_{\max} = \max\{y_{S_1}, \ldots, y_{S_N}\}$ into Δ_2.
   (c) Repeat (a) and (b) M times.
3) Compute the initialization of $\widehat{\Theta}_K^{(0)}$, i.e.,

$$\begin{aligned} \widehat{\sigma}_{i,K}^{(0)} &= \widehat{\sigma}_{i,K-1} \qquad \forall i \in \{1, 2, \ldots, K-1\} - \{m\} \\ \widehat{\sigma}_{m,K}^{(0)} &= \sum_{y_s\in\Delta_1} y_s/M \\ \widehat{\sigma}_{K,K}^{(0)} &= \sum_{y_s\in\Delta_2} y_s/M. \end{aligned} \tag{13}$$

When $K = 1$, the initialization of $\widehat{\Theta}$ is computed from the whole image Y, and $\widehat{\lambda}_K^{(0)} = 0.5$ is experimentally selected.

This initialization scheme imposes the parameter estimation $\widehat{\Theta}_{K-1}$ to iteratively compute $\widehat{\Theta}_K$, according to minimizing the inner variance of the clusters.

D. RAMRF Clustering Algorithm Flow

The proposed RAMRF clustering method is designed in a two-loop way.

1) Outer loop: The outer loop determines the cluster number using the PLIC. In every iteration of this loop, first, it initializes $\widehat{\Theta}$, as described in Section IV-C, then updates the $\widehat{W}$ by the inner loop until convergence, and finally computes and compares $\mathrm{PLIC}(K)$ with $\mathrm{PLIC}(K-1)$ for choosing the first local maximum of $\mathrm{PLIC}(K)$ to end the outer loop.

2) Inner loop: The inner loop is to estimate the optimal $\widehat{\Theta}$ under fixed cluster number K and is designed in a "hard" membership EM style: in the E step, with fixed parameters, the optimal data clusters are rapidly searched, minimizing (9) by the GC, under the criterion of MAP; and in the M step, the parameters are estimated, as described in Section IV-B, using current data clusters obtained in the E step with hard membership. The two steps are iterated until the inner loop converges.

The algorithm flowchart of the RAMRF is shown in Fig. 1.

The RAMRF clustering method is obviously different from existing methods with the following characteristics. 1) Unlike the classical clustering methods (e.g., K-means and FCM) and their variations, our method imposes the spatial information in the feature space by embedding an MRF in it. In this way, the method can improve the clustering precision. 2) Unlike conventional USMRF-based segmentation methods, which usually use "soft" cluster membership (means probability) for data, the RAMRF clustering method adopts "hard" membership, that is to say, a pixel will be assigned a class label with probability 1 or 0 for it being or not being in the cluster. The "soft" way in the conventional MRF-based methods may make the parameter estimation described in Section IV-B more effective, but it must sample a probability for the clusters in every E step (for instance, SA or Swendsen–Wang cut [16] can be used to sample the probability), which makes the cluster estimation more difficult and even intractable, leading to expensive computation. However, when using the "hard" cluster membership here, the RAMRF clustering method can organize every

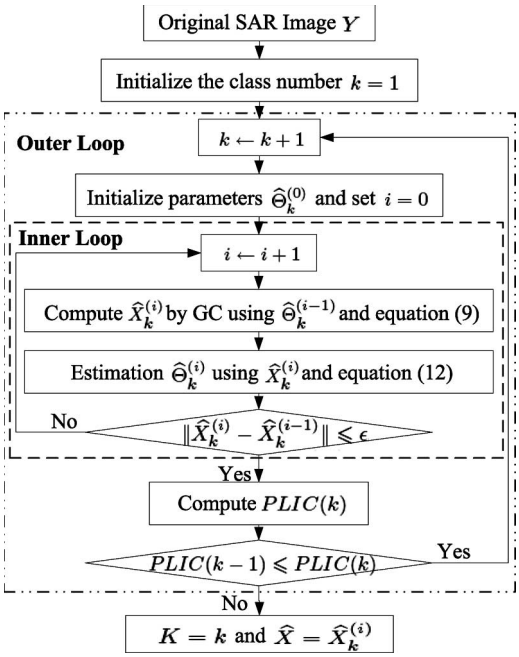

Fig. 1. Flowchart of the proposed RAMRF clustering method.

E step as a graph partition step, and this graph partition problem can be rapidly solved by the GC. It eases the computation burden and benefits the energy minimization. 3) The proposed algorithm can automatically work, without giving the cluster number and any parameter, which is different from the first two characteristics. 4) Our method runs more quickly with higher clustering precision than the traditional MRF-based clustering methods.

V. Experimental Results

The performance of the RAMRF clustering method is tested on both simulated and real SAR images. To effectively illustrate the precision and computational time of the proposed algorithm, we make some comparisons among the RAMRF clustering method, the classical clustering method, i.e., K-means, and the traditional USMRF-based SAR image segmentation method.

First, to illustrate the clustering precision of the RAMRF clustering method, we test the proposed algorithm on a sequence of simulated images with the same parameter $\Theta = \{[150\ 260\ 430\ 690\ 900\ 1300\ 2200\ 3100], 0.5\}$ but different looks, i.e., with different SNR [as in the SAR images, the number of looks $L = mean(Y)/\sqrt{var(Y)}$]. Fig. 2(a) is the ground truth of the simulated image sequence and Fig. 2(b) is a three-look simulated image in the sequence. We apply the three methods, K-means clustering method with SAR spatial image filtering beforehand (in this letter, the Lee speckle filter is used), USMRF-based SAR image segmentation method (the method in [7] is adopted), and our RAMRF clustering method, to this image sequence. Here, the cluster number in the former two methods is assigned to be 8, which is the true cluster number, as they cannot be determined by the algorithms themselves. In the inner loop of RAMRF clustering method, ϵ is set to be 0.5% of the total number of pixels in the image. The precision curves of the three methods are shown in Fig. 3, and for the three-look image shown in Fig. 2(b), the precisions are 87.45% of the K-means clustering method, 95.12% of the traditional USMRF-based method, and 96.10% of the RAMRF clustering method.

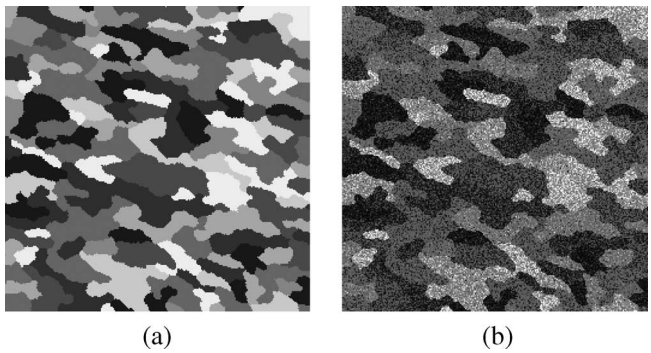

Fig. 2. Ground truth for the sequence of simulated SAR images (size: 256 × 256). (a) Ground truth with eight classes. (b) A three-look simulated SAR image in the sequence.

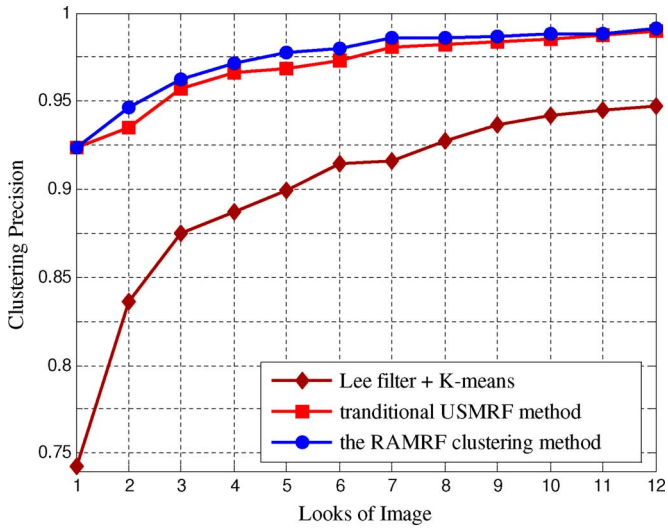

Fig. 3. Comparisons on the clustering precision. These curves are obtained on a sequence of simulated SAR images with the same eight-cluster ground truth and their looks ranging from 1 to 12. We can see that the RAMRF clustering method overperforms the traditional USMRF-based method and K-means on precision.

Second, the three methods are also tested on a sequence of images with the sizes of $[40 \times 40, 60 \times 60, \ldots, 250 \times 250]$. The curves for the computational time of the three methods running on this image sequence are shown in Fig. 4.

The comparisons in Figs. 3 and 4 show that the proposed RAMRF clustering method can automatically, rapidly, and robustly cluster the SAR image with high precision.

Fig. 5(a) is a four-look L-band polarimetric SAR image (HV channel) with the size of 374 × 374, which was acquired from an agricultural land scene in Flevoland (Netherlands). The clustering results of the three methods are shown in Fig. 5(b)–(d). Fig. 5(b) is the clustering result obtained by K-means with Lee filtering beforehand. Fig. 5(e)–(g) shows the edge images of clustering results in Fig. 5(b)–(d), respectively. The clustering results and their edge images of the three methods show that the RAMRF clustering method provides more regular and precise result than the other two methods do.

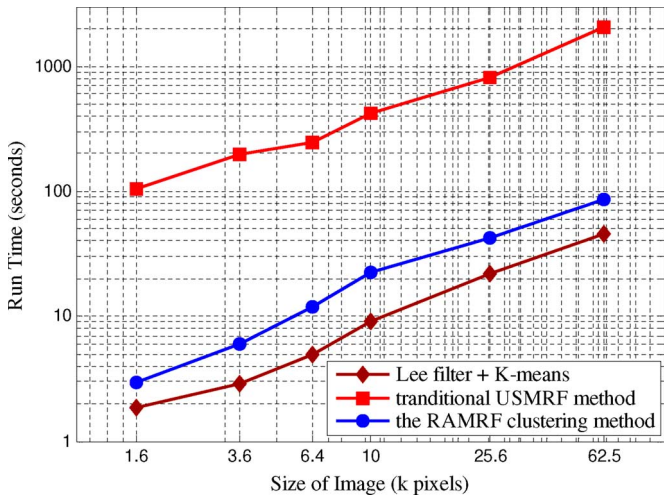

Fig. 4. Comparisons on running time. The three different methods are applied to different simulated SAR images with sizes of $[40 \times 40, 60 \times 60, \ldots, 250 \times 250]$. The experiments are performed on a 2.8-GHz Pentium IV personal computer with 1-GB random access memory. We can see that the RAMRF performs faster than the traditional USMRF-based method but slower than K-means with Lee filtering beforehand.

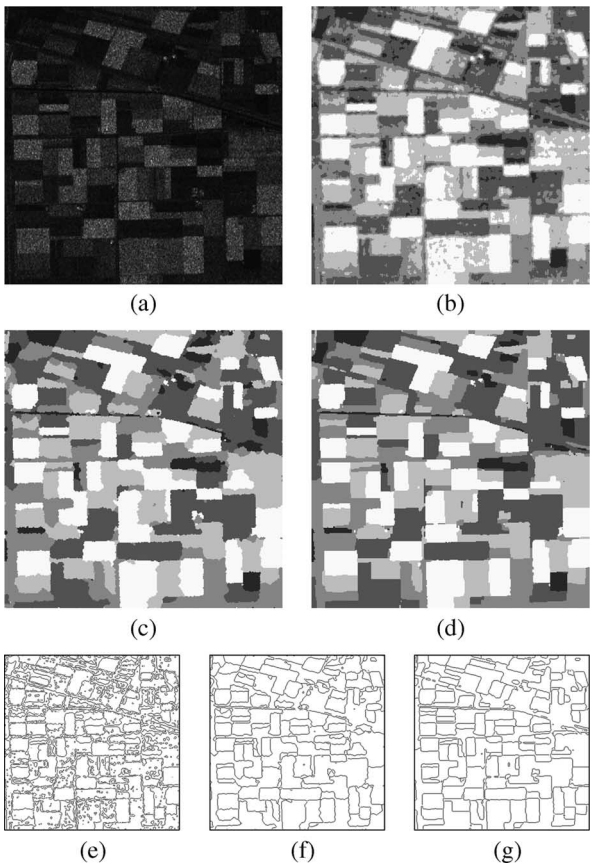

Fig. 5. Clustering comparison experiments on real SAR image. (a) Four-look Jet Propulsion Laboratory's L-band polarimetric SAR image (HV channel) with the size of 374 × 374, which was acquired from an agricultural land scene in Flevoland (Netherlands). (b) Clustering result of K-means with Lee filtering beforehand, given the cluster number $K = 5$. (c) Clustering result by the traditional USMRF-based SAR image segmentation method, given the cluster number $K = 5$. (d) Clustering result by the proposed RAMRF clustering method in this letter. (e)–(f) are edge images of (b)–(d), respectively. The clustering results and their edge images of the three methods show that the RAMRF clustering method gives more regular result than the other two methods do.

VI. Conclusion

In this letter, we present a rapid and automatic clustering method for SAR images by embedding an MRF model in the clustering space and using the multilevel GCs to effectively compute the optimal clusters for the data. The clustering method is approximately global optimal in the sense of MAP. The robustness of the RAMRF clustering algorithm both on precision and computational time are test on two sequence of images with different SNR and sizes, respectively. Experiments both on simulated and real SAR images show that the proposed method has impressive performance. The clustering result can be taken as a precise scene classification or an input for higher SAR image interpretation.

Acknowledgment

The authors would like to thank Y.-L. Guo and C.-M. Xiong for their valuable discussion.

References

[1] R. O. Duda, P. E. Hart, and D. G. Stork, *Pattern Classification*, 2nd ed. New York: Wiley, 2001, pp. 517–583.
[2] S. Geman and D. Geman, "Stochastic relaxation Gibbs distributions, and the Bayesian restoration of images," *IEEE Trans. Pattern Anal. Mach. Intell.*, vol. PAMI-6, no. 6, pp. 721–741, Jun. 1984.
[3] B. S. Manjunath and R. Chellappa, "Unsupervised texture segmentation using Markov random fields," *IEEE Trans. Pattern Anal. Mach. Intell.*, vol. 13, no. 5, pp. 478–482, May 1991.
[4] A. Sarkar, M. K. Biswas, B. Kartikeyan *et al.*, "A MRF model-based segmentation approach to classification for multispectral imagery," *IEEE Trans. Geosci. Remote Sens.*, vol. 40, no. 5, pp. 1102–1113, May 2002.
[5] G. Poggi, G. Scarpa, and J. B. Zerubia, "Supervised segmentation of remote sensing images based on a tree-structured MRF model," *IEEE Trans. Geosci. Remote Sens.*, vol. 43, no. 8, pp. 1901–1911, Aug. 2005.
[6] H. Deng and D. A. Clausi, "Unsupervised segmentation of synthetic aperture radar sea ice imagery using a novel Markov random field model," *IEEE Trans. Geosci. Remote Sens.*, vol. 43, no. 3, pp. 528–538, Mar. 2005.
[7] Y. Cao, H. Sun, and X. Xu, "An unsupervised segmentation method based on MPM for SAR images," *IEEE Geosci. Remote Sens. Lett.*, vol. 2, no. 1, pp. 55–58, Jan. 2005.
[8] Y. Yang, H. Sun, and C. He, "Supervised SAR image MPM segmentation based on region-based hierarchical model," *IEEE Geosci. Remote Sens. Lett.*, vol. 3, no. 4, pp. 517–521, Oct. 2006.
[9] Y. Boykov, O. Veksler, and R. Zabih, "Fast approximate energy minimization via graph cuts," *IEEE Trans. Pattern Anal. Mach. Intell.*, vol. 23, no. 11, pp. 1222–1239, Dec. 2001.
[10] Y. Boykov and V. Kolmogorov, "Experimental comparison of min-cut/max-flow algorithms for energy minimization in computer vision," *IEEE Trans. Pattern Anal. Mach. Intell.*, vol. 26, no. 9, pp. 1124–1137, Sep. 2004.
[11] V. Kolmogorov and R. Zabih, "What energy functions can be minimized via graph cuts?" *IEEE Trans. Pattern Anal. Mach. Intell.* vol. 26, no. 2, pp. 147–159, Feb. 2004.
[12] C. S. Derek and E. R. Adrian, "Approximate Bayes factors for image segmentation: The pseudolikelihood information criterion (PLIC)," *IEEE Trans. Pattern Anal. Mach. Intell.*, vol. 24, no. 11, pp. 1517–1520, Dec. 2002.
[13] R. E. Kass and A. E. Raftery, "Bayes factors and model uncertainty," *J. Amer. Stat. Assoc.*, vol. 90, pp. 773–795, 1995.
[14] H. Maitre, *Traitement Des Images De Radar à Synthèse D'ouverture*. Paris, France: Paris-Collection IC2, 2001, pp. 10–50.
[15] H. Derin and H. Elliot, "Modeling and segmentation of noisy and textured images using Gibbs random fields," *IEEE Trans. Pattern Anal. Mach. Intell.*, vol. PAMI-9, no. 1, pp. 39–55, Jan. 1987.
[16] A. Barbu and S. C. Zhu, "Generalizing Swendsen–Wang to sampling arbitrary posterior probabilities," *IEEE Trans. Pattern Anal. Mach. Intell.*, vol. 27, no. 8, pp. 1239–1253, Aug. 2005.